

# Low Loss Tunable Filters in Substrate Integrated Waveguide

S. Sirci, J. D. Martínez, M. Taroncher and Vicente E. Boria

Instituto de Telecomunicaciones y Aplicaciones Multimedia,  
Universitat Politècnica de València,  
8G Building - access D - Camino de Vera s/n - 46022 Valencia (Spain)  
Corresponding author: [ssirci@iteam.upv.es](mailto:ssirci@iteam.upv.es)

## Abstract

In this work, the design and experimental results of compact low-loss filters, based on the extension of the classical coaxial waveguide resonator to Substrate Integrated Waveguide technology, are successfully demonstrated. The design, fabrication and measurement of a continuously tunable cavity resonator and a two-pole filter at S-band in single-layer SIW technology are presented. These structures keep the low-cost fabrication scheme of single-layer PCB processing, while requiring less than half the area compared to a conventional SIW design.

**Keywords:** Tunable filters, varactor tuning diodes, combline resonator, compact filter design, microwave filter, continuous tuning, Substrate Integrated Waveguide (SIW).

## 1. Introduction

The concept of Substrate Integrated Waveguide (SIW) has been developed to synthesize waveguide cavities with planar structures into a single dielectric material, combining integrated high Q-factor filters with low cost fabrication techniques. A SIW component consists on a synthetic waveguide formed by the top and the bottom metal plates of a dielectric slab and is bounded transversely by two sidewalls of cylindrical metallic via-holes. The rows of vias connect top and bottom metal layers forming the cavity walls. Input and output coupling is achieved using tapered microstrip transmission lines or coplanar current probes. Adjusting the geometrical dimensions of the taper or probes, the input/output coupling can be controlled.

The SIW components can be fabricated on printed circuit boards (PCBs) or low-temperature co-fired ceramics (LTCCs) technologies. They enable a significant reduction of size, weight and cost compared with metallic waveguide designs. As the SIWs are based in the  $TE_{n0}$  modes, the characteristic of conventional waveguides are preserved and the propagation of energy of these modes is substantially limited in the substrate. Thus, they have a higher Q-factor and lower loss than other planar guided-wave structures, for instance microstrip lines and coplanar waveguides (CPW). In fact, conventional planar resonators provide a moderate unloaded Q-factor, typically less than  $Q_u < 100-200$ , while SIW resonators can reach a Q-factor higher than 500 using low-loss substrates. Furthermore, a growing interest has also focused on SIW technology because they can be easily integrated with microstrip or coplanar waveguide circuits [1] on the same laminate.

Traditionally, the adaptive function of the front-end preselection filters is achieved using a bank of switchable fixed frequency filters for multiple frequency bands [2]. However, this means that both the size and cost increase, due to the complexity of the filter structures. Recently, due to their potential to reduce system size and complexity, tunable filters are called to be key components in the future microwave communication subsystems, particularly in the development of future multi-band multi-standard miniaturized front-ends. This trend has led to the increased demand for filter technologies with frequency tunable ability. Therefore, in the design of low-loss reconfigurable filters, the availability of high-Q tunable resonators is of primary concern. While frequency and bandwidth tunability have been extensively demonstrated in planar technology using different tuning elements (e.g. varactor diodes [3], ferroelectrics [4] or MEMS [5, 6]), an increasing interest has

**The availability of high-Q tunable resonators is of primary concern in the design of low-loss reconfigurable filters which are called to be key components in the future microwave communication subsystems.**

grown on electronically tunable SIW cavity resonators as an enabling technology for the design of very low-loss tunable filters [7, 8] that can be an alternative to filter banks in several applications.

In this paper we present a novel structure for implementing high-Q frequency agile resonators based on combline SIW cavities loaded with GaAs varactor tuning diodes. Following this concept, the design of compact and continuously tunable filters based on a combline topology is presented. The resonators and filters are fabricated in a low-cost microwave substrate using a conventional single-side PCB fabrication process and off-the-shelf GaAs varactors.

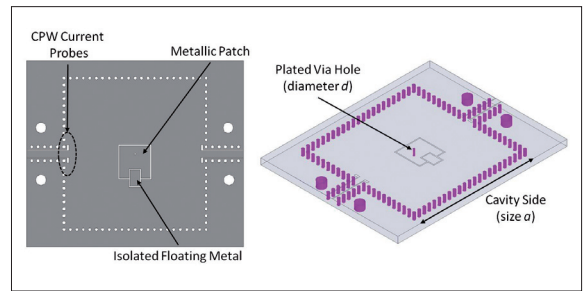
Some previous research has been very recently done in the study of reconfigurable SIW structures [9-11], concerning mainly the design of discretely tunable filters. A first attempt of using perturbing conductive elements for tuning the resonant frequency of a SIW cavity was proposed in [9], although no experimental device was then reported. More recently, a PIN diode-based discretely tunable SIW resonator consisting on switchable perturbing elements has been proposed [10]. Finally, a different approach for center frequency tuning of multi-layer filters has made use of relatively large piezoelectric actuators disks with remarkable results, however at the price of a more sophisticated design [11].

In this paper we propose a continuously tunable SIW filter based on a combline topology. Then, an S-band combline filter is successfully designed, fabricated and measured. Experimental and simulation results are in good agreement, showing the potential advantages of this structure in terms of size and design flexibility, without increasing insertion losses compared to its conventional SIW counterpart. The main advantages of our structure are the following: continuous tuning range, more compact design, negligible power consumption and low-cost fabrication process. Moreover, a model for the proposed resonator is considered, and a systematic procedure for the design of these miniaturized coupled resonator bandpass filters is presented.

## 2. Combline Tunable Resonator in SIW Technology

### 2.1 Resonator Structure

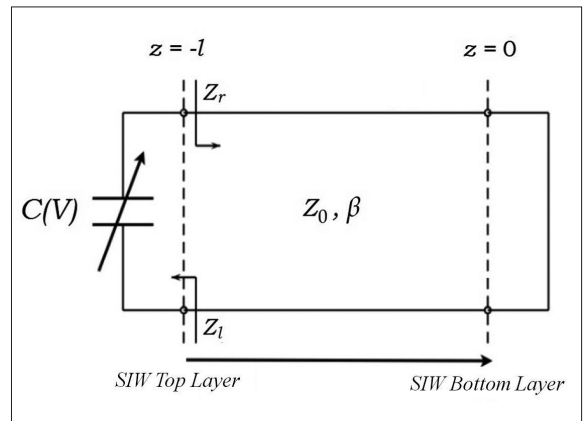
The structure of the tunable combline SIW resonator is shown in Fig. 1. It consists on a square cavity (size  $a$ ) where a conducting post has been inserted at the center of the resonator using a plated via hole. A metal patch connected to that post and separated from the SIW top



■ **Figure 1.** Drawing of the resonator, showing the conducting post and the floating and metal patches.

plate by a small gap is created on the top side of the cavity. So, the inner via is short-circuited at the bottom metallic plan and open ended at the top. A loading capacitance  $C_0$  is therefore established between the post and the top metal layer of the SIW through the fringing fields across the annular gap.

Thus, the proposed resonator can be seen as a square-circular coaxial waveguide cavity, and can be modeled as a piece of TEM mode transmission line short-circuited at one end and capacitively terminated at the other. A scheme of the equivalent circuit is shown in Fig. 2.

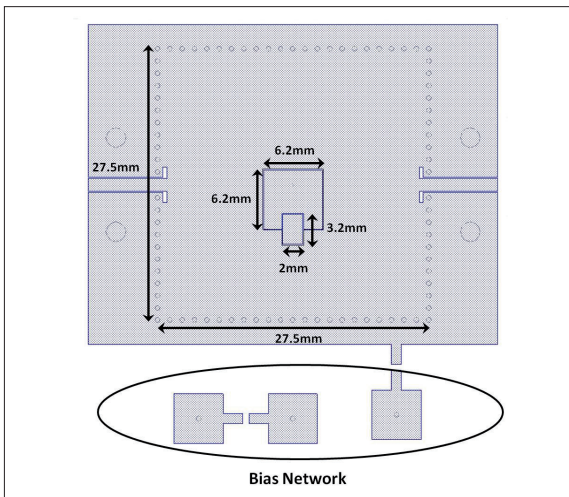


■ **Figure 2.** Equivalent circuit of the combline SIW resonator loaded at the capacitive end with a tuning varactor diode.

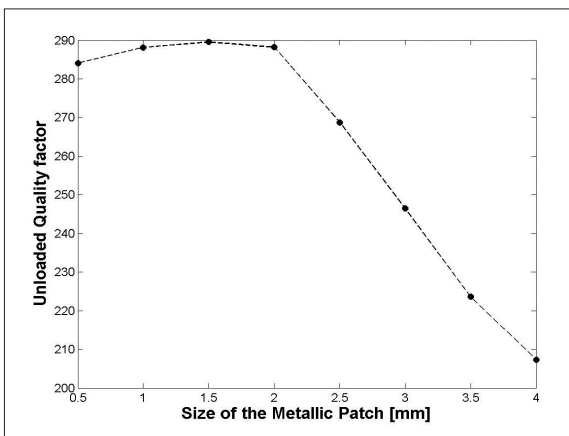
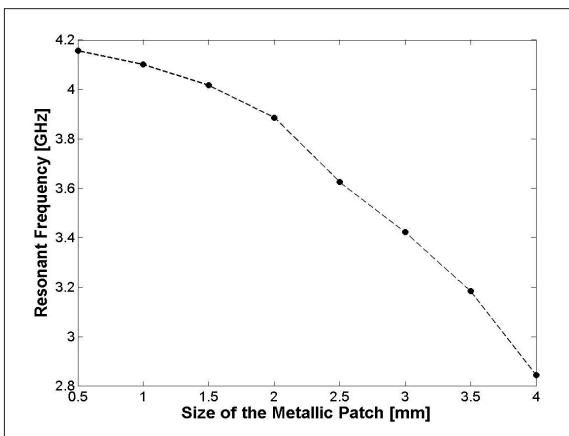
Due to the previous model, the resonant frequency of the SIW combline resonator can be expressed as a function of the substrate thickness  $l$ , the annular gap capacitance  $C_0$  and the characteristic impedance of the rectangular-circular coaxial waveguide  $Z_0$ .

In order to validate the proposed concept, we have studied the tuning range and unloaded quality factor of a tunable combline SIW resonator. Firstly, a device about 4 GHz has been designed using full-wave 3D simulation of the structure using HFSS. The dimensions of the designed resonator can be seen in Fig. 3. It is worth pointing out that the excitation of the resonator is performed through magnetic coupling through CPW probes.

As shown, the resonant frequency  $f_R$  is not only a function of the width and length of the cavity, but also a func-



■ **Figure 3.** Layout of the designed resonator. Via hole and conductive post diameters are 0.5 and 0.3 mm respectively. Metal patch gap is 0.1 mm.



■ **Figure 4.** Change in resonant frequency  $f_R$  (left) and  $Q_0$  (right) as a function of the size  $a$  of metallic patch.

tion of size  $a$  of the metallic patch, the isolating gap and the diameter of the central conducting post. These properties of the combline resonator can be used to reduce the resonant frequency, without a significant decreasing in the  $Q$  factor of the resonator.

Fig. 4(a) and 4(b) show the dependence of  $f_R$  and unloaded  $Q_0$  factor on the dimensions of the central patch for

the proposed combline resonator on  $\epsilon_r = 3.55$  substrate. It is seen that a high percentage change of the  $f_R$  can be obtained changing the length  $a$  between 2 and 3 mm, with low degradation of  $Q_0$  factor.

## 2.2 Tuning Element

The resonant frequency of the filter can be controlled by changing the loading capacitance  $C_0$  of the combline resonator as shown in Fig. 5. Thus, GaAs varactor diodes have been inserted connected to the metal patch for modulating the capacitance of the resonator.

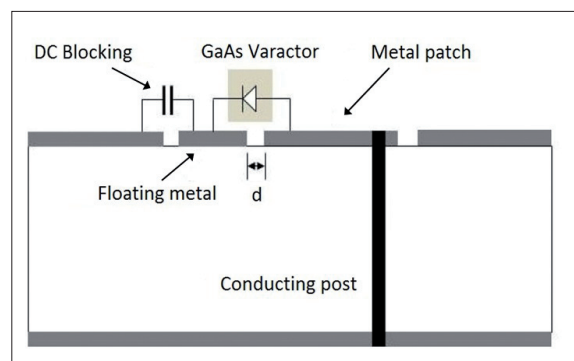
A hyper-abrupt junction GaAs varactor has been used in this work as tuning element. Particularly, we have chosen the MA46H200 from MA-COM. It exhibits a capacitance variation from 0.25 to 1 pF for a reverse bias voltage between 22 and 0 V respectively. The nominal  $Q$ -factor at 50 MHz is 3000 giving an estimated series resistance of 2.2  $\Omega$ .

An important advantage of using tuning varactors instead of switching elements (i.e. PIN diodes) is the negligible power consumption of the device while operating in reverse bias conditions. Moreover, the need of only one varactor per cavity significantly reduces the complexity of the bias network.

## 2.3 Continuously Tunable Resonator

The loading capacitance  $C_0$ , that would initially include the capacitance between the metal patch and the SIW top plate, can be controlled by inserting a varactor connecting both sides. In order to simplify the biasing and optimizing the varactor RF performance, a floating metal island (it can be seen in Fig. 5) is created between the metal patch and the SIW top plate.

The cathode of the varactor is then connected to this floating pad while a series capacitor is inserted between the former and the top metal side of the cavity for providing a low impedance path for the microwave signal. The series DC blocking capacitor has been chosen of 1.5 pF in order to slightly reduce the capacitive effect of the varactor and improve a little bit the unloaded  $Q_0$  of the reso-

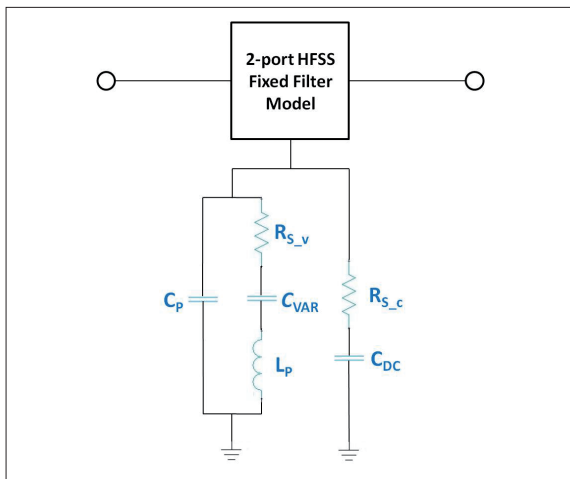


■ **Figure 5.** Drawing of the cross-section of the combline resonator. The varactor is connected between the island and the metal patch.

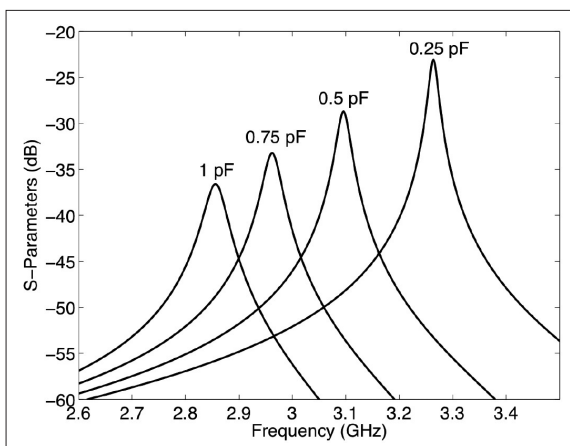
nator. We have chosen to keep the varactor bias circuit as simple as possible, so a thin wire has been connected from the floating metal island to a bias pad. Thus, a convenient bias voltage can be applied between the floating pad and the top metal of the SIW cavity by using this thin wire. DC bias and ground connections have been isolated by using high value resistors (i.e.  $R > 100 \text{ k}\Omega$ ), specifically  $1 \text{ M}\Omega$  resistors have been used.

Then, internal ports have been created at the places where the varactor and the fixed capacitance will be inserted in order to combine 3D EM simulations with circuit simulations using the equivalent models of the lumped components. The equivalent circuit model of the tunable combline resonator is shown in Fig. 6, including parasitic components for the varactor diode and the DC blocking capacitance.

The resonator has been strongly under-coupled (i.e. the  $S_{21}$  parameter has been kept below  $-20 \text{ dB}$ ) in order to enable us the accurate measurement of the unloaded  $Q$  factor from the transmission response of the device [12]. Simulations for different values of varactor capacitance have been carried out. The simulated results are shown in Fig. 7.



■ **Figure 6.** The equivalent circuit model of the tunable resonator used in circuit simulations.



■ **Figure 7.** Simulated results of the under-coupled tunable SIW resonator for different values of varactor capacitance.

The estimated unloaded  $Q_0$  ranges from 180 to 70 for a capacitance variation between  $0.25 \text{ pF}$  and  $1.25 \text{ pF}$ . For the same capacitance range, the resonance frequency changes from  $3.3 \text{ GHz}$  to  $2.8 \text{ GHz}$ . Thus, an estimated tuning range about  $15\%$  can be extracted from the obtained results. The nominal parasitic due to the varactor packaging and the series capacitor have been included in the simulations.

### 3. Filter Design in SIW Technology

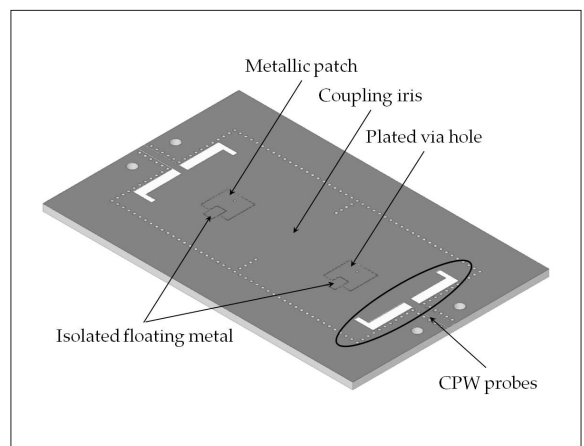
#### 3.1 Combine Filter

For high- $Q$  filter, it is critical to achieve center frequency tuning without degrading the  $Q$  factor of the filter. Since tunable lumped components are generally low  $Q$  at microwave frequency, they will decrease the overall quality factor. The proposed tunable structure allows the possibility of employing low- $Q$  varactors or high- $Q$  MEMS varactors to achieve center frequency control, with slightly degradation of the overall  $Q$ , as shown in the previous chapter.

The structure of a 2-pole combline filter in SIW technology can be seen in Fig. 8. The filter consists of two tunable SIW resonators, coupled by irises. In fact, narrow  $n$ -order bandpass filters can be implemented by inserting inductive windows coupling adjacent resonators.

Each resonator consists on a square/circular SIW cavity of side  $a$  where a plated via hole has been inserted at the center of the resonator, where the electromagnetic field of the fundamental mode is maximum. This inner via is short-circuited at the bottom side and connected to a metal patch electrically isolated from the top side through a small gap.

A capacitive effect is therefore established between this metal patch and the top plane of the SIW. This capacitance value depends on the perimeter of the metal patch, the spacing of the gap and the thickness of the metallization layer.



■ **Figure 8.** Scheme of the 2-pole combline filter in SIW technology.

For the input/output couplings to the resonators, we have maintained the same structure of previous combline resonator. These are performed by means of coplanar waveguide CPW probes as shown in Fig.8. Therefore, the external coupling can be therefore controlled by the geometrical dimensions of the probes. The inter-resonators coupling is controlled by means of irises created on the adjacent walls. Since the diameter of the rows of via holes is considered fixed, the coupling level can be adjusted changing the size of the iris and the distance between iris via holes.

As shown, the proposed tunable SIW resonator can be seen as a TEM square-circular coaxial transmission line of length  $h$  (i.e. the substrate height) short-circuited at one end and capacitively terminated at the other. The susceptance  $\beta(\omega)$  of the coaxial resonator can be expressed as

$$\beta(\omega) = \omega C_0 Y_0 \cot(\beta h) \quad [1]$$

Where,  $C_0$  is the total capacitance of the central metal patch,  $Y_0$  the characteristic admittance of the TEM mode short-circuited transmission line formed by the inner (circular) and outer (rectangular) conductor,  $h$  the substrate thickness and the phase constant of the coaxial line at frequency  $\omega$  is

$$\beta = \frac{\omega \sqrt{\epsilon_r}}{C_0} \quad [2]$$

Where,  $\epsilon_r$  is the dielectric permittivity of the substrate, while  $C_0$  is the speed of light in vacuum. Now, the resonant frequency of the SIW cavity can be computed from the equation  $\beta(\omega) = 0$ , that is

$$\omega C_0 = Y_0 \cot\left[\frac{\omega \sqrt{\epsilon_r}}{C_0} h\right] \quad [3]$$

The inductive contribution comes from the TEM mode short-circuited resonator, which can be seen as a short piece of coaxial transmission line of length and characteristic admittance embedded into the dielectric material of permittivity  $\epsilon_r$ . For a circular inner conductor of diameter  $d$  and a square contour of side  $a$ , the characteristic admittance can be well approximated when  $a \gg d$  by [13]

$$Y_0 = \left[ \frac{60}{\sqrt{\epsilon_r}} \ln\left[1.079 \frac{a}{d}\right] \right]^{-1} \quad [4]$$

Finally, from [14], the capacitance established between the metal disk of radius and the SIW top metal can be computed. It is worth mentioning, the thickness of the metallic layers is not considered in this expression.

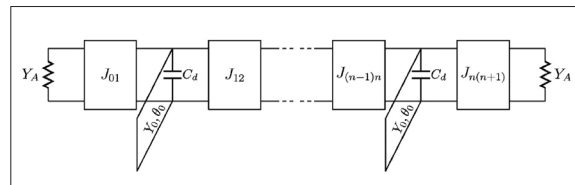
### 3.2 Filter Design

The synthesis and dimensioning of the tunable filter is performed by the classical approach for directly coupled resonator filters. Firstly, the low-pass prototype parameters  $g_0, g_1, \dots, g_{n+1}$  are computed from the desired response. From

**The proposed resonator can be seen as a square-circular coaxial waveguide cavity, and can be modeled as a piece of TEM mode transmission line short-circuited at one end and capacitively terminated at the other.**

these values, the external quality factor  $Q_{ext}$  and inter-resonator coupling coefficients  $K_{ij}$  are obtained from the well-known expressions [12]. Secondly, a SIW combline resonator at the center frequency of the filter is designed taking into account the dielectric constant  $\epsilon_r$  and the substrate thickness  $h$ . The side of the square SIW cavity and the diameter of the inner via will determine the  $Y_0$  value of the coaxial resonator. Additionally, the dimension of the metal patch and the isolating gap width control the loading capacitance  $C_0$ .

The prototype of the combline bandpass filter can be mo-



■ **Figure 9.** Equivalent prototype of an  $N^{th}$ -order combline resonator bandpass filter with frequency invariant admittance inverters.

deled using shunt resonators and frequency-invariant admittance inverters, as shown in Fig. 9. Given a filter response with centre frequency and bandwidth, being and the upper and lower cutoff frequencies, the loading capacitance and the admittance of the coaxial resonator can be obtained by mapping the resonator susceptance and the admittance inverters of the bandpass filter with those of the low-pass prototype. The former condition can be expressed as

$$\beta(\omega) = \omega' \left[ \frac{b \frac{\Delta\omega}{\omega_0}}{\Omega_c} \right] \quad [5]$$

Where  $b$  is the resonator slope parameter,  $\omega'$  and  $\Omega_c = 1$  rad/s the angular frequency and cut-off frequency of the low-pass prototype respectively. The level of  $b$  will impact the unloaded  $Q$  factor of the resonator, and must be a trade-off between low losses, compactness and feasibility of the synthesized values of  $C_0$  and  $Y_0$ .

Now, substituting (1) into (4) for the corresponding pass-band edge frequencies  $\omega' = \pm 1 \rightarrow \omega = \{\omega_H, \omega_L\}$  we can obtain

$$C_0 = \left[ \frac{b \frac{\Delta\omega}{\omega_0}}{\Omega_c} \right] \frac{\cot\theta_H + \cot\theta_L}{\omega_H \cot\theta_L - \omega_L \cot\theta_H} \quad [6]$$

And



$$Y_0 = \left[ b \frac{\Delta\omega}{\omega_0} \right] \frac{\omega_H + \omega_L}{\omega_H \cot\theta_L - \omega_L \cot\theta_H} \quad [7]$$

Finally, the admittance inverters can be computed from the low-pass prototype coefficients using the well-known expressions

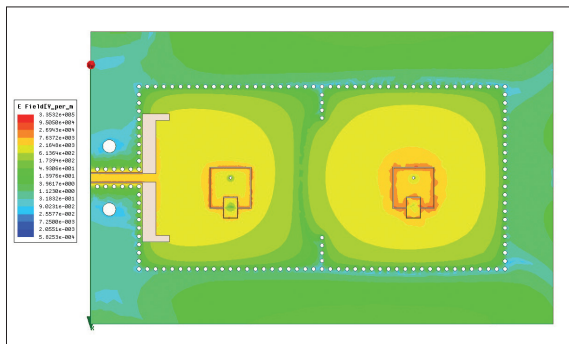
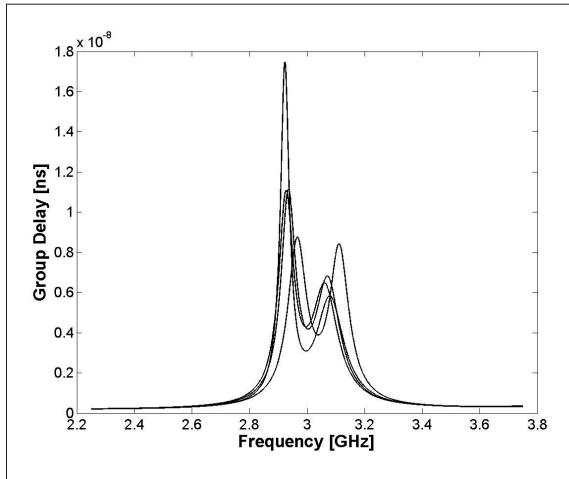
$$J_{0,1} = \sqrt{\frac{Y_A \left[ b \frac{\Delta\omega}{\omega_0} \right]}{g_0 g_1}} \quad J_{n,n+1} = \sqrt{\frac{Y_A \left[ b \frac{\Delta\omega}{\omega_0} \right]}{g_n g_{n+1}}}$$

$$J_{i,i+1} = \left[ b \frac{\Delta\omega}{\omega_0} \right] \sqrt{\frac{1}{g_i g_{i+1}}} \quad [8]$$

For  $i = 1$  to  $(n - 1)$ , where  $Y_A$  is the admittance of the input/output access ports.

Following this approach, a 2-pole Chebyshev filter centered at 3.1 GHz with 5% fractional bandwidth will be synthesized. Once the SIW cavity resonator has been designed, the values of  $Q_{ext}$  and  $K_{ij}$  are computed as a function of the input/output CPW probe dimensions and the width of the coupling irises using 3D full-wave simulations with HFSS software, as shown in Fig. 10.

In order to match the desired response of the filter, the resonators are tuned from the reflection group delay res-

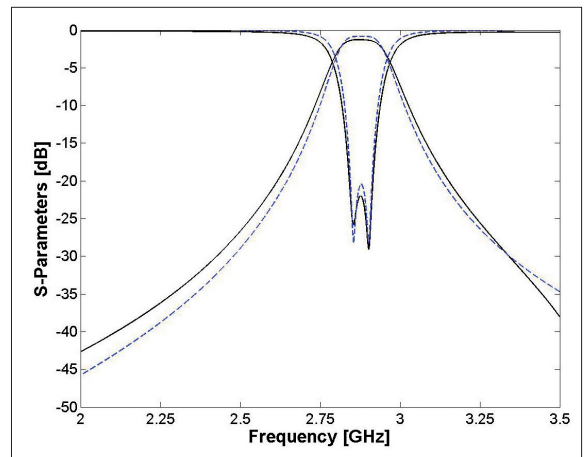


■ **Figure 10.** Simulated results of the group delay (left) as a function of dimensions of the coupling iris, and intensity of the electromagnetic field (right).

ponse of short-circuited cavities. For adjusting the centre frequency, the dimensions of the central square post or the size of the cavities are modified. Moreover, by changing the diameter of the inner vias the central frequency can be coarsely adjusted.

A final optimization of the filter dimensions is then performed for the minimum capacitance value of the tuning element, combining 3D full-wave results with circuitual simulations using the equivalent models of the lumped components. As previous exposed, in the 3D model of the circuit, internal ports have been created at the places where the varactors 46H200 (from MA-COM) and the fixed capacitance will be inserted.

Since all the parameters are now determined, the simulated response of the designed filter can be obtained using ANSOFT Designer and is shown in Fig. 11. The minimum capacitance of the varactor (0.25 pF) has been chosen to run this simulation. The centre frequency of the complete bandpass filter is 2.88 GHz and the insertion loss is estimated less than 1.5 dB.



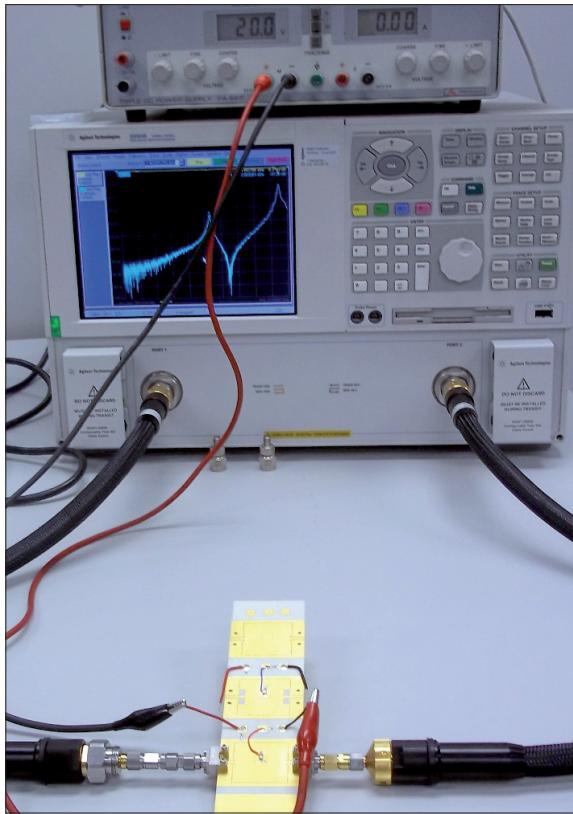
■ **Figure 11.** Simulated results of the design filter (thick) and ideal response (dashed) for a minimum varactor capacitance of 0.25 pF.

## 4 Experimental Results

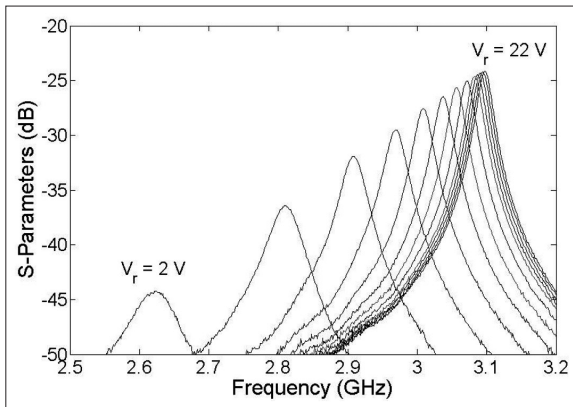
### 4.1 Fabrication and Measurement of Tunable SIW Resonator

A prototype of the resonator has been fabricated using Rogers RT/Duroid 4003C laminate ( $\epsilon_r = 3.55$  and  $\tan \delta = 2.7 \cdot 10^{-3}$ ). A picture of the fabricated device including the biasing wires is shown in Fig. 12. The size of the resonator is  $27 \times 27 \text{ mm}^2$ , showing an important size reduction compared to its equivalent conventional SIW counterpart due to the capacitive loading of the metal patch.

The measured  $S_{21}$  parameters for the tunable combine SIW resonator are shown in Fig. 13. A tuning range of almost 20% is observed when changing the reverse bias voltage of the varactor from 2 to 22 V.



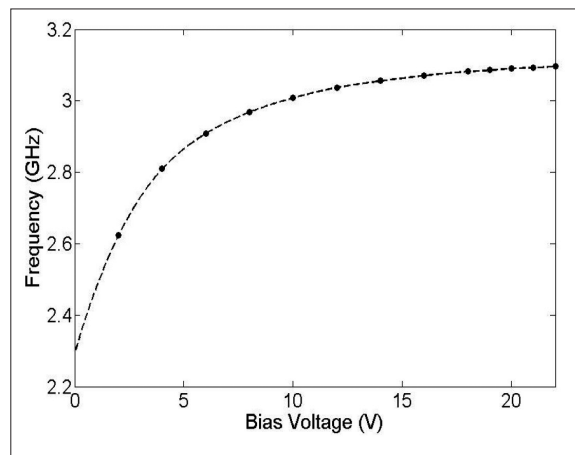
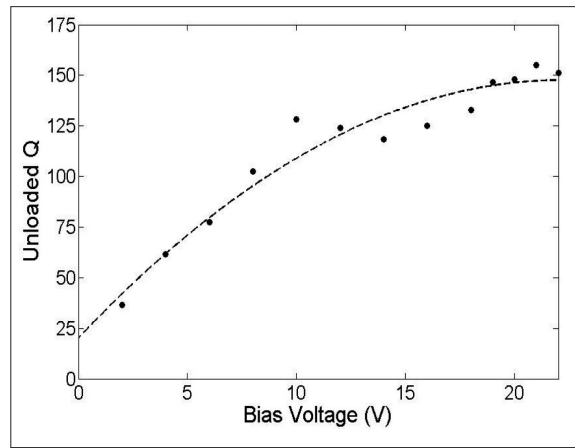
■ **Figure 12.** Photography of the fabricated device under measurement.



■ **Figure 13.** Simulated results of the under-coupled tunable SIW resonator for different values of varactor capacitance.

The resonant frequency and the unloaded  $Q$  of the resonator as a function of the reverse bias voltage are shown in Fig. 14. As can be seen, the tunable  $Q$  of the resonator ranges from 40 to 150, being above 100 for the first 200 MHz of frequency shift. The power consumption of the device is negligible along the whole tuning voltages (i.e. typically less than 1  $\mu$ W).

Although, the percentage value of tuning range is similar to estimated value, the range of frequency has moved to lower frequencies, since it ranges from 3.1 GHz to 2.6 GHz. The differences with the simulated results are attributed to an underestimation of the capacitance between the metal patch and the floating island where the



■ **Figure 14.** Resonance frequency (right) and unloaded  $Q$  (left) of the tunable resonator as a function of the reverse voltage applied to the varactor.

DC bias is applied. This effect slightly increases the total loading capacitance, decreasing both the resonant frequency of the structure and the achievable tuning range of the resonator. Fabrication and permittivity tolerances contribute also to the small shift to lower frequencies of the response. The small increase of losses between experimental and simulated results is attributed to the mounting and soldering of the components.

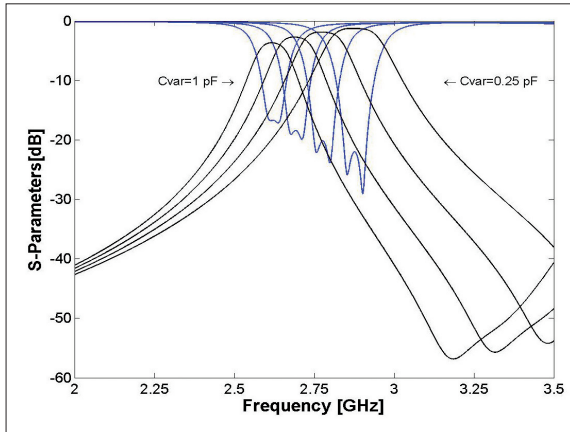
#### 4.2 Fabrication and Measurement of Tunable SIW 2-pole Filter

To validate our filter topology, a 2-pole bandpass Chebyshev filter was designed, fabricated and measured in 1.524 mm-thick Rogers RO4003C substrate. The fixed combline filter is first designed with equiripple fractional bandwidth of 5%, center frequency of 3.1 GHz while the requested in-band return losses are  $-20$  dB. Simulation results of the tunable filter for the whole varactor capacitance range can be seen in Fig. 15.

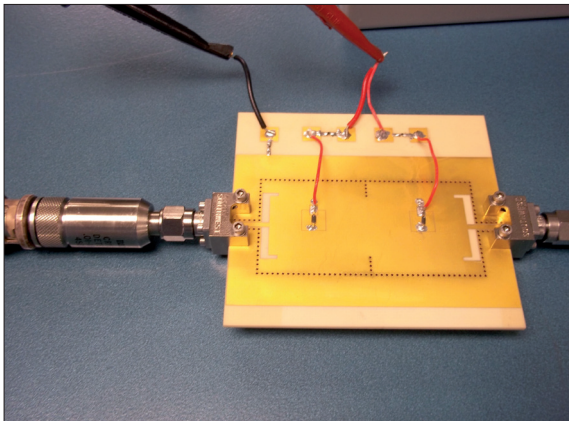
The prototype was fabricated using standard single-layer PCB processing technology. The layout and dimensions of the fabricated filter is depicted in Fig. 16. Filter size are  $55 \times 27.5$  mm<sup>2</sup>, while the equivalent conventional SIW filter would require about twice the area for square cavities using the dominant TE<sub>101</sub> mode.

**Main advantages of combine SIW tunable filter are the following: continuous tuning range, negligible power consumption, more compact design and low-cost fabrication process.**

The input/output CPW lines present a trace width of 1.3 mm and a ground plane spacing of 0.15 mm, so the characteristic impedance is closed to  $50 \Omega$ . The diameter of the vias for the SIW cavities and irises is  $600 \mu\text{m}$ , and the



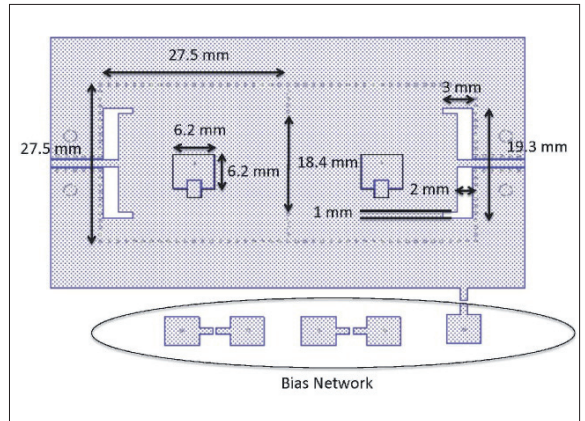
■ **Figure 15.** Simulation results of the fabricated filter for a varactor capacitance ranging from  $0.25 \text{ pF}$  ( $f_0 = 2.88 \text{ GHz}$ ) to  $1 \text{ pF}$  ( $f_0 = 2.64 \text{ GHz}$ ).



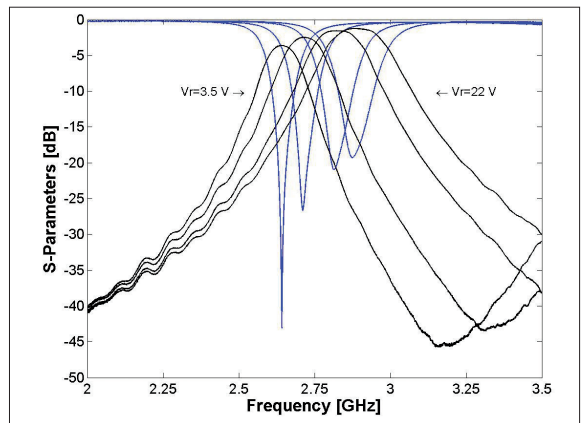
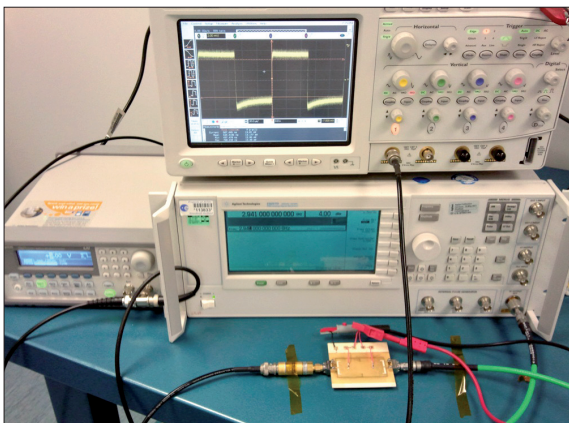
spacing between the contour vias is  $1.25 \text{ mm}$ . The central via hole presents a diameter of  $300 \mu\text{m}$  and the metal patch isolating gap is  $100 \mu\text{m}$ . Photography of the fabricated filter and the measured S-parameters are shown in Fig. 17.

Measured results agree quite well with the simulations. The device centre frequency can be tuned between  $2.64$  and  $2.88 \text{ GHz}$  for a bias voltage ranging from  $3.5 - 22 \text{ V}$ . The insertion losses vary from  $1.27 \text{ dB}$  to  $3.63 \text{ dB}$  across the whole tuning range. Moreover, a variation of the  $3\text{-dB}$  fractional bandwidth between  $4\% - 7\%$  has been observed due to the short length of the coaxial resonator. The tuning range of the proposed approach is mainly limited by the moderate  $Q$ -factor of the tuning elements and the frequency dependence of the input/output and inter-resonators couplings. However, the more compact design would enable us to integrate several switchable reconfigurable filters in order to cover a broader frequency band. Moreover, the use of higher  $Q$  tuning elements (e.g. MEMS switches and varactors) will allow an increase of the tuning range without degrading the EM performance of the device.

The presence of the varactor introduces non-linearity effects that limit the power handling of the filter. Results of intermodulation distortion and linearity of the fabricated filter can be seen in Fig. 18. It is worth mentioning

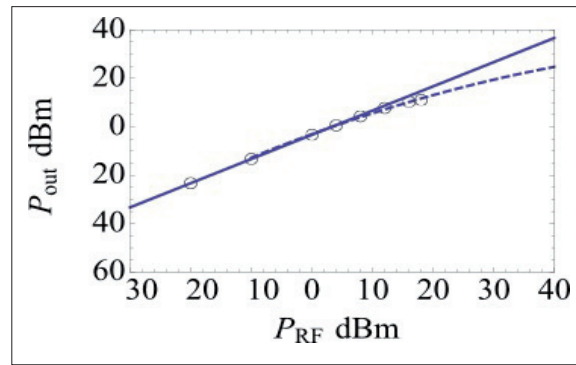
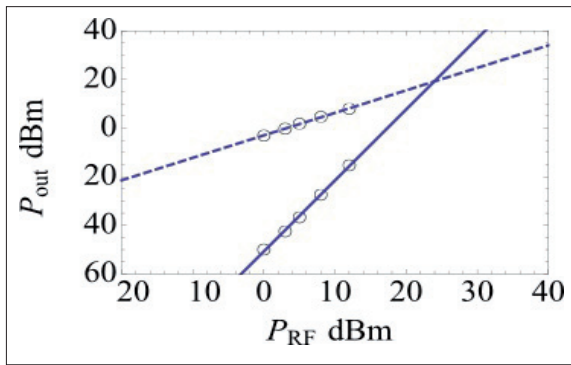


■ **Figure 16.** (Left): Photography of the tunable filter during the  $1\text{-dB}$  compression point measurement. (Right): Layout and dimensions of the fabricated tunable filter.



■ **Figure 17.** (Left): Photography of the tunable filter during the reconfiguration time measurement. (Right): Measured S-parameters of the fabricated tunable 2-pole filter.





■ **Figure 18.** (Left): Results of two-tone third-order intermodulation (thick) intercept point IIP3. (Right): Measured filter output power as a function of the input carrier level.

that these effects have been measured for the worst-case of a high varactor capacitance.

Thus, a two-tone third-order intermodulation intercept point (IIP3) of +24 dBm has been measured for a bias voltage  $V_b = 5$  V and a two-tone separation  $\Delta f = 50$  kHz. However, the 1-dB compression point of the filter at the same bias voltage is only +10 dBm.

The reconfiguration time of the filter has been measured using a crystal power detector at the filter output and a 4 dBm tone centered at 2.85 GHz at the input. Then, the bias voltage has been changed between 20 and 14 V with a 100  $\mu$ s-period square signal. The measurement setup is shown in Fig. 17. The low-to-high and high-to-low measured reconfiguration times of the filter are 120 and 720 ns for a centre frequency shift about 40 MHz.

## 5 Conclusions

A tunable combline SIW resonator has been proposed in this paper. The capacitively loaded end of the resonator has been used in order to include a surface-mounted tuning varactor diode that changes the resonant frequency of the device. A  $Q$ -factor better than 100 has been obtained for a 200 MHz tuning range from 3.1 GHz. The proposed device can be fabricated using a low-cost PCB process and using off-the-shelf GaAs varactor diodes. The structure presents a continuous tuning range of almost 20% and negligible power consumption.

The obtained results are very promising compared to typical planar tunable resonators [3, 5, 6], while other SIW tunable cavities based on semiconductor tuning elements have achieved unloaded  $Q$ 's around 100 on a discretely tunable approach [10]. Moreover, losses due to the tuning element could be significantly reduced by using RF MEMS varactors.

A continuously tunable filter has been designed, fabricated and measured in SIW technology. Main advantages of the proposed structures are analog tuning range, low losses and easy integration with other planar circuits. Additionally, due to the combline topology of the devices,

a very compact implementation is also achieved with a very wide spurious-free band. This approach shows interesting applications for the design of low-loss tunable filters based on compact high- $Q$  SIW resonators. Moreover, the application of this technology to the post-manufacturing tuning of narrow-band SIW filters could be studied showing promising results. The design, performance and manufacturability of novel combline filters in SIW technology have been demonstrated. The measured results show an excellent agreement with the EM simulations when all involved physical effects are considered. The proposed topology presents important advantages in terms of size compactness, spurious rejection and design flexibility.

## Acknowledgments

The authors would like to thank Generalitat Valenciana and MICINN (Spanish Government) for its financial support under projects GV/2009/007 and TEC2010-21520-C04-01.

## References

- [1] D. Deslandes and K. Wu, "Single-substrate integration technique of planar circuits and waveguide filters", *IEEE Trans. Microwave Theory & Tech.*, vol. 51, no. 2, pp. 593-596, Feb. 2003.
- [2] D. Packiaraj, V.S. Reddy, G.J. Mello, and A.T. Kalgatgi, "Electronically switchable suspended substrate stripline filters", in *Proc. RF and Microwave Conference*, pp. 64-66, Oct 2004.
- [3] I.C. Hunter, and J.D. Rhodes, "Electronically tunable microwave bandpass filters", *IEEE Trans. Microwave Theory & Tech.*, vol. 30, no. 9, pp. 1354-1360, Sept. 1982.
- [4] J. Nath, D. Ghosh, J.P. Maria, A.I. Kingon, W. Fathelbab, P.D. Franzon, and M.B. Steer, "An electronically tunable microstrip Bandpass filter using thin-film barium-strontium-titanate (BST) varactors", *IEEE Trans. Microwave Theory Tech.*, vol. 53, no. 9, pp. 2707-2712, Sept. 2005.
- [5] A. Pothier, J.-C. Orlianges, E. Zheng, C. Champeaux, A. Catherinot, D. Cros, P. Blondy, and J. Papapolymerou, "Low loss two bit tunable bandpass filters using MEMS

- dc contact switches", IEEE Trans. Microwave Theory Tech., vol. 53, no. 1, pp. 354 – 360, Jan. 2005.
- [6] I. C. Reines, A. R. Brown, and G. M. Rebeiz, "1.6-2.4 GHz RF MEMS tunable 3-pole suspended combline filter", in IEEE MTT-S Int. Microwave Symp. Dig., Atlanta, GA, June 2008, pp. 133-136.
- [7] D.W. Winter, and R. R. Mansour, "Tunable Dielectric Resonator Bandpass Filter with Embedded MEMS Tuning Elements", IEEE Trans. Microwave Theory Tech., vol. 55, no. 1, pp. 154-159, Jan. 2007.
- [8] F. Huang, and R.R. Mansour, "Tunable Compact Dielectric Resonator", 39th European Microwave Conference, 2009, EuMC 2009, Rome, Italy, pp. 559-562, Oct. 2009.
- [9] J. C. Bohorquez, B. Potelon, C. Person, E. Rius, C. Quendo, G. Tanne, and E. Fourn, "Reconfigurable planar SIW cavity resonator and filter," in IEEE MTT-S Int. Dig., vol. 3, pp. 947–950, Jun. 2006.
- [10] M. Armendariz, V. Sekar and K. Entesari, "Tunable SIW bandpass filters with PIN diodes", Proc. 40th European Microwave Conference, Paris, France, pp. 830-833 Oct 2010.
- [11] H. Joshi, H.H. Sigmarsson, S. Moon, D. Peroulis, and W.J. Chappell, "High-Q fully reconfigurable tunable bandpass filters", IEEE Trans. Microwave Theory Tech., vol. 57, no. 12, pp. 3525-3533, Dec. 2009.
- [12] J.S. Hong and M.J. Lancaster, "Microstrip Filter for RF/Microwave Applications", New York, NY: John Wiley & Sons, Inc., 2001.
- [13] H. J. Riblet, "An accurate approximation of the impedance of a circular cylinder concentric with an external square tube," IEEE Trans. Microwave Theory Tech., vol. MTT-31, no. 10, pp. 841–844, Oct. 1983.
- [14] H. S. Lee and H. J. Eom, "Potential distribution through an annular aperture with a floating inner conductor," IEEE Trans. Microwave Theory Tech., vol. 47, no. 3, pp. 372–374, Mar. 1999.

## Biographies



**Stefano Sirci** was born in Torino, Italy. He received the B.S. and M.S degrees in Electronic Engineering from the University of Perugia, Perugia, Italy, in 2006 and 2009, respectively. He is current working toward the PhD degree at the Universitat Politècnica de València, Valencia, Spain.

Since 2009, he has been with the Microwave Application Group (GAM) at the Institute of Telecommunications and Multimedia Applications (iTEAM) at the Universitat Politècnica de València. His research interest is currently focused on designing, fabrication and measurement of tunable microwave filter in substrate integrated waveguide (SIW) technology.



**Jorge D. Martínez** received the Ingeniero de Telecomunicación and the Doctor Ingeniero de Telecomunicación degrees from the Universitat Politècnica de València, Valencia, Spain, in 2002 and 2008. He joined the Department of Electronic Engineering of the Universitat Politècnica de València in 2002, where he is Associate Professor since 2009. He was a Visiting Researcher at XLIM (Centre National de la Recherche Scientifique / Université de Limoges) from June 2006 to September 2007, working on the design and fabrication of radio-frequency microelectromechanical systems (RF MEMS). His current research interests are focused on emerging technologies for reconfigurable microwave components with emphasis on tunable filters and RF MEMS.



**Mária Taroncher (S'03)** was born in Llíria, Valencia, Spain, on October 8, 1979. She received the Telecommunications Engineering degree from the Universidad Politècnica de Valencia (UPV), Valencia, Spain, in 2003, and is currently working toward the Ph.D. degree at UPV.

From 2002 to 2004, she was a Fellow Researcher with the UPV. Since 2004, she has been a Technical Researcher in charge of the experimental laboratory for high power effects in microwave devices at the Research Institute iTEAM, UPV. In 2006 she was awarded a Trainee position at the European Space Research and Technology Centre, European Space Agency (ESTEC-ESA), Noordwijk, The Netherlands, where she worked in the Payload Systems Division Laboratory in the area of Multipactor, Corona Discharge and Passive Intermodulation (PIM) effects. Her current research interests include numerical methods for the analysis of waveguide structures and the acceleration of the electromagnetic analysis methods.



**Vicente E. Boria** received the Ingeniero de Telecomunicación and the Doctor Ingeniero de Telecomunicación degrees from the Universitat Politècnica de València, Valencia, Spain, in 1993 and 1997. In 1993 he joined the Universitat Politècnica de València, where he is Full Professor since 2003. In 1995 and 1996

he was held a Spanish Trainee position with the European Space research and Technology Centre (ESTEC)-European Space Agency (ESA). He has served on the Editorial Boards of the IEEE Transactions on Microwave Theory and Techniques. His current research interests include numerical methods for the analysis of waveguide and scattering structures, automated design of waveguide components, radiating systems, measurement techniques, and power effects in passive waveguide systems.